

BEAM PROFILE MEASUREMENTS WITH A SLIT-FARADAY CUP AND A WIRE SCANNER FOR A NEWLY DEVELOPED 18 GHZ SUPERCONDUCTING ECR ION SOURCE AND ITS LEBT*

H. J. You[#], S. O. Jang, and W. I. Choo, NFRI, Gunsan, Korea

Abstract

In this presentation we show results of beam profile measurements by a slit-Faraday cup and a wire scanner. Argon 8+ beams were generated in a new liquid helium-free superconducting electron cyclotron resonance ion source (ECRIS). The ECRIS, named SMASHI, was successfully developed at the National Fusion Research Institute in 2014, and in the future it will be dedicated for highly charged ions matter interaction research facility (HIMIRF). Before designing HIMIRF terminals after low energy beam transport (LEBT), it is necessary to characterize the beam properties of the source and its LEBT line. The beam profile measurements have been done after an analyzing dipole magnet (DM). The slit-Faraday cup and the wire scanner were installed at 25 cm and 120 cm from the exit flange of the DM, respectively. Between the two diagnostics an Einzel lens was positioned to control the focusing of diverged beams. Here, with the measurements we checked the present beam alignments in the LEBT, and studied the dependence of beam profile variation on the operations of beam optics such as steering magnets and Einzel lens.

INTRODUCTION

A new superconducting 18 GHz electron cyclotron resonance ion source and its low energy beam transport were developed at the National Fusion Research Institute in South Korea [1]. The source, named SMASHI (Superconducting Multi-Application Source of Highly-charged Ions), will be dedicated for future application of highly charged ions in the area of matter interaction, diagnostic imaging, and probing. In this proceeding, we briefly describe SMASHI and its LEBT. Then, we show preliminary results of beam charge spectra of ^4He , ^{16}O , ^{40}Ar , ^{132}Xe ion beams. In order to characterize the beam properties in the LEBT, we also measured beam profiles by a slit-FC system and a wire scanner, by which the beam alignments of the source and the LEBT are checked. Variations of beam profiles are studied with respect to different settings of ion optics in the LEBT.

SOURCE DESCRIPTION

Figure 1 shows the overall section view of SMASHI. As an ECRIS for generating multiply/highly-charged ions, SMASHI has following main features: two-frequency heating (18, 18+ Δ GHz), high power-capable

plasma chamber, remotely-positional variable gap extraction system, capability to generate a wide range of ion elements from gas to metal, and two diagnostic ports for the extraction region. All these features are highly oriented to the generation of diverse highly charged ions (HCI). Most of all, due to the helium-free SC magnet, SMASHI can be more economically operated with low power consumption, which therefore enabling the full system of ECRIS operated on a high-voltage platform.

Microwave Injection

In Fig. 1, the microwave injection side can be viewed. Normally, the injection electrode is located at the maximum position of the axial magnetic field, and depending on the source condition it can be moved to other optimum positions by adjusting the bellows. In the injection electrode two WR62 waveguide ports, an on-axis sputtering hole, a centered-perforated biased disk, two diagnostic/oven holes, and one gas hole were arranged [1]. The WR62 ports, placed well out of the plasma pattern, are separated by 120° from each other. The biased disk is shaped as a triangle with a thru-hole in its center, into which the on-axis sputtering target is inserted. The sputtering target system is remotely positional and designed to easily exchange different materials.

Extraction System

The extraction system, shown in Fig. 1, is a puller-Einzel lens system consisting of 3 electrodes. Each electrode is supported and guided by 4 rods fixed to the extraction chamber. The distance between electrodes can be adjusted when necessary. The whole extraction system is remotely positional by a motor-driven-control, where the gap between the plasma electrode and the puller electrode is adjustable by 20–50 mm. Table 1 summarizes the extraction conditions and beam characteristics. The resulted rms emittance for Ar^{8+} was calculated by using IGUN with the inclusion of the magnetic field and charge state distribution (CSD). The resulting beam radius and the momentum of Ar^{8+} beam are 33 mm and 41 mrad, respectively.

Table 1: Extraction Conditions and Beam Characteristics

Extraction voltage	30 (10-30) kV
Gap distance	33 (20-50) mm
Einzel lens (negative)	30 (10-30) kV
Rms emittance for Ar^{8+} at 500 mm from plasma electrode	48 mm mrad ($R_{\text{max}}=33$ mm, $A_{\text{max}}=41$ mrad)

*This work was supported by R&D Program of ‘Plasma Convergence & Fundamental Research’ through the National Fusion Research Institute of Korea (NFRI) funded by the Government funds
#hjyou@nfri.re.kr

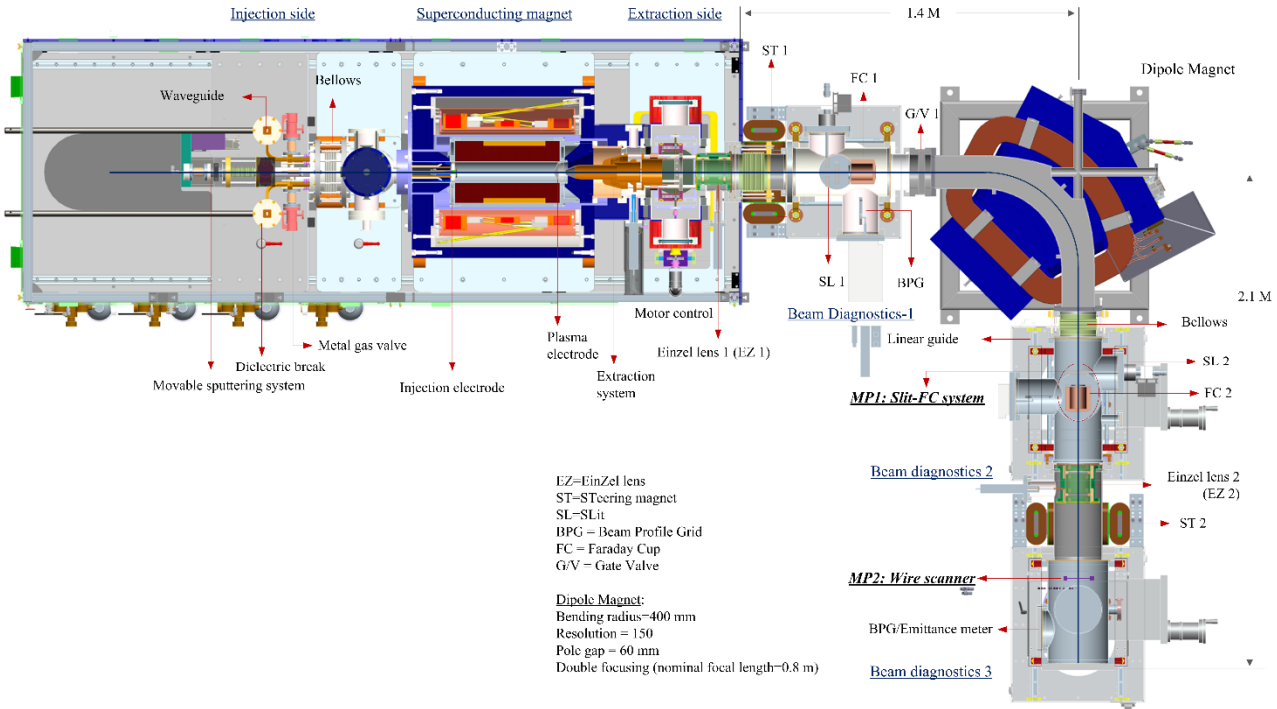


Figure 1: A sectional layout of the NFRI 18 GHz superconducting ECR ion source (SMASHI) & its LEBT.

Magnetic Structure

The magnet system of SMASHI consists of four superconducting(SC) coils sets and a permanent hexapole. The SC coils is designed to be cooled by a single cryocooler (1.5W at 4.2 K) and give axial mirror fields of $B_{inj} = 2.0$ T and $B_{ext} = 1.4$ T, where B_{inj} and B_{ext} are the peak fields in the microwave injection region and the beam extraction region, respectively. The hexapole is created by 36 pieces of permanent magnets and gives a radial mirror field of $B_{rad} = 1.3$ T. Figure 2 shows the magnet design, and Table 2 summarize the main parameters of the magnet. The more detailed design, cooling, and excitation results are found in references [2, 3]

Table 2: Main Parameters Of The Magnet System

B_{inj}	1.7-2.0 T
B_{ext}	1.3-1.4 T
B_{ecr}	0.65 T
B_{rad}	1.3 T
B_{min}	0.4-0.5 T
Superconducting wire	NbTi(Cu) 1.25×0.8 mm for coil 1-3, Ø 0.5 mm for coil 4
Cryocooler	Single GM cryocooler (1.5 W @ 4.2 K/45 W @ 60 K)
Permanent hexapole	36 pieces of NdFeB magnets

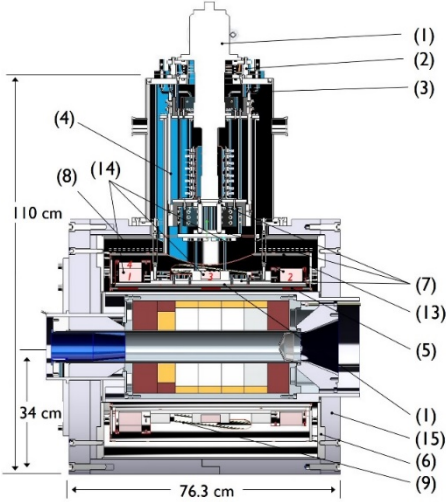


Figure 2: Magnet structure of SMASHI: (1) OFHC bobbin, (2) Superconducting coils, (3) two-step thermal links, (4) HTS lead, (5) copper thermal shield, (6) multilayer superinsulation sheets, (7) thermal insulating supports, (8) vacuum casing, (9) iron yoke, (10) current leads, (11) α -gel anti-vibration, (12) cryocooler, and (13) quench detection loop.

LEBT

Low energy beam transport (LEBT) is designed for the resent 18 GHz superconducting ECR ion source. A sectional layout of the LEBT is shown in the right side of Fig. 1. The LEBT is composed of 5 sections: Einzel lens, beam diagnostics 1(BD-1), double focusing dipole magnet (DM), beam diagnostics 2, and 3 (BD-2, -3). In

the beam line of the LEBT, extracted ion beams are diagnosed by a Faraday cup (FC) and/or beam profile grid, then specific mass and charge state of beam is selected by the DM. After the DM, the species analysed beam can be profile-monitored by a slit-FC system and a wire scanner in BD-2 and BD-3, respectively. The Einzel lens 1, located just after the extraction system, helps to focus the diverged beam, so that it could go parallel to the DM and be focused at slit 2(SL2). In BD-1, a high power FC are installed for measuring the total ion beam current from the source. The DM is a 90° analysing magnet (double focusing) of which bending radius, pole gap, magnetic rigidity, and mass resolution of the DM are 400 mm, 60 mm, 0.36 Tm, and 150, respectively. The inlet and the outlet dimensions of the DM vacuum chamber are both 135 wide and 52 mm high. Bellows inserted before and after the DM are installed to provide good connectivity and beam matching. BD-2 just after the DM also consists of a beam slits (horizontal and vertical) and a FC. A horizontal(x) and a vertical(y) slit can operate to limit the beam divergence and envelope, and they also play a role of analyzing slits in the slit-FC system for beam profile measurement. Thereafter, Einzel lens 2 is installed between BD-2 and BD-3 to re-focus the beam. Steering magnets (ST 1 and ST 2) can be used before and after the DM in case beam paths need to be adjusted.

In Fig. 3 an example of beam envelope calculations is shown. The calculations are done by Trace 3-D Module with electrostatic palette in PBO Lab 3.2.5. The input parameters for Trace 3-D was based on a measured beam current and beam charge spectra. The input emittance value is get from IGUN calculation.

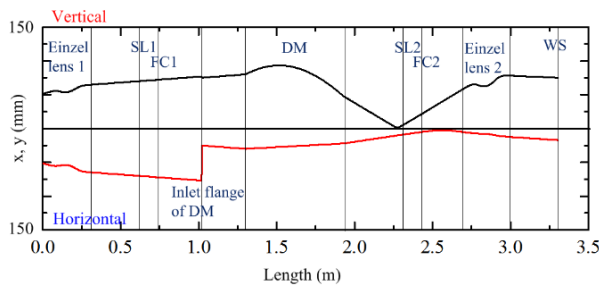


Figure 3: Horizontal and vertical envelopes of Ar^{8+} ion beam in the LEBT.

PRELIMINARY RESULTS OF SMASHI

As the first commissioning results of SMASHI, beam charge spectra of ^4He , ^{16}O , ^{40}Ar , and ^{132}Xe ion beams and their intensities are measured. The results are drawn in Fig. 4. So far, the source were operated under the following conditions: Maximum TWT power was limited to 600 W (+300 W). Injection B-field was fixed to 1.7 T (80 % of full intensity). The aperture of plasma electrode and the extraction voltage are Ø8 mm and Max. 20 kV, respectively. The position of the biased disk are optimally adjusted between 10 to 40 mm from the end of the injection electrode, and its biased voltage was -200 to -600 V. Note that, during the operation conditions, we

intentionally reduce the microwave power and/or magnetic field level so that the x-ray emission from the source do not exceed the safe dose level of 0.5 $\mu\text{Sv/h}$ (at operator position). Until the end of this year, the source shielding will be more strengthened. Though all available operating knobs could not be fully used due to the safety issue from X-ray emission, the performances of SMASHI are promising and will be dramatically enhanced by applying higher microwave power(>1000 W/liter), higher magnetic field (>2 T), extraction potential up to 30 kV, and optimum position of plasma electrode, and improved LEBT transmission.

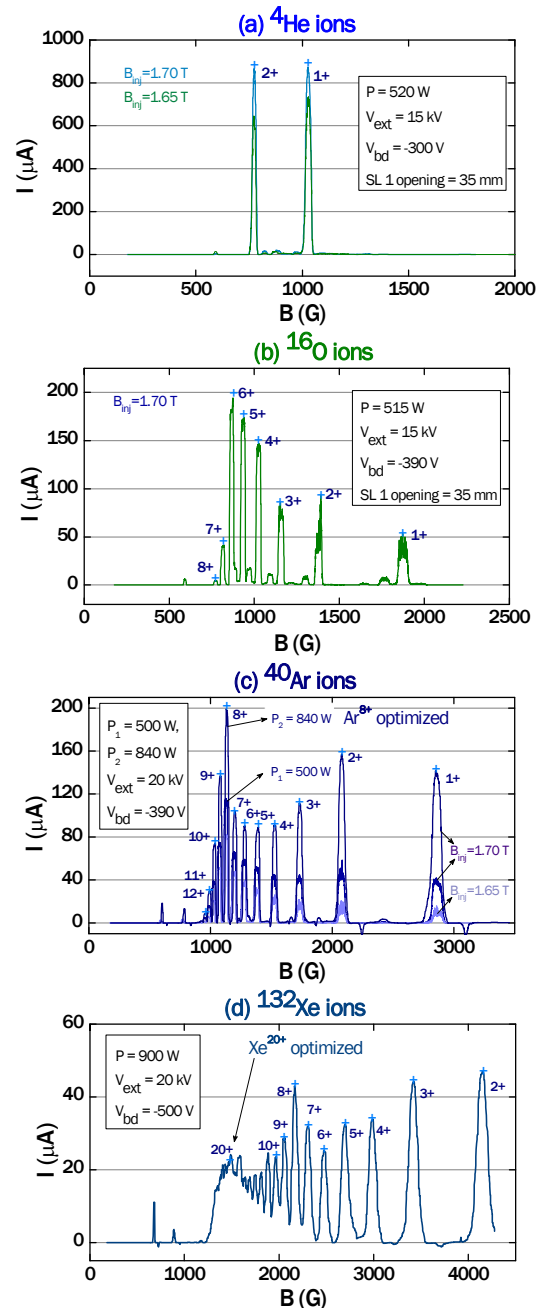
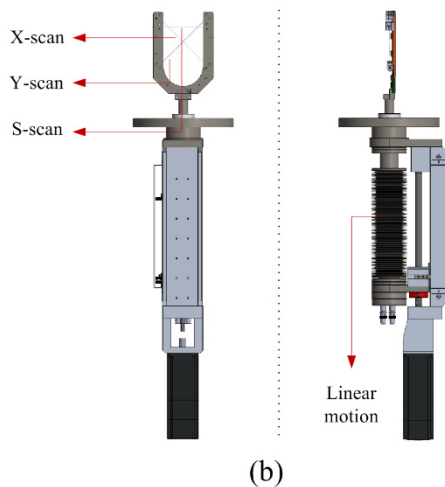
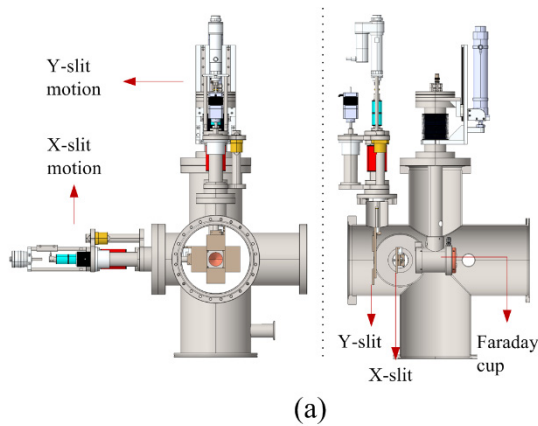


Figure 4: Beam charge spectra of ^4He , ^{16}O , ^{40}Ar , ^{132}Xe ion beams from SMASHI.

BEAM PROFILE MEASUREMENT

For BPM, as shown in Fig. 5(a), the x and y slit in the slit-FC system are designed to be independently movable from -25 to 25 mm. Also the gap widths(d 's) of the slits are remotely controllable from 0 to 50 mm. When the slit-FC system works for BPM, the gap width of a moving slit is normally set to 2.5 mm, and the other one is set to 50 mm. In other words, when horizontal(x) beam profile is measured, x slit of $d=2.5$ mm is moved from $x=-25$ to 25 mm while y slit is fixed at $y=0$ with its gap width set to 50 mm. The FC is comprise of an isolated metal cup and a high voltage suppression ring close to the entrance of the cup. The cup is $\varnothing 50$ mm in diameter and 80 mm in length, and the suppression ring can be biased up to -1 kV.

The wire scanner (WS), shown Fig. 5(b), is a fork type scanner. The WS is inserted into the beamline by an angle of 45 degree. The WS is composed of three wires mounted in horizontal(x), vertical(y), and diagonal(s) directions, so that three directions of profiles can be simultaneously measured by one passage. The scanning length of the WS was designed to be 165 mm; The measurement ranges of x, y, and s direction become 50(-25 to 25 mm), 50(-25 to 25 mm), 95 mm(-42.5 to 42.5 mm), respectively.



Beam profile measurements have been done at the positions MP 1 and MP2 (see Fig. 1), which are respectively 25 and 116 cm away from the exit flange of DM. Here target ion beam was selected to be Ar^{8+} . TWT microwave power was set to 300 W. The Ar^{8+} beam was

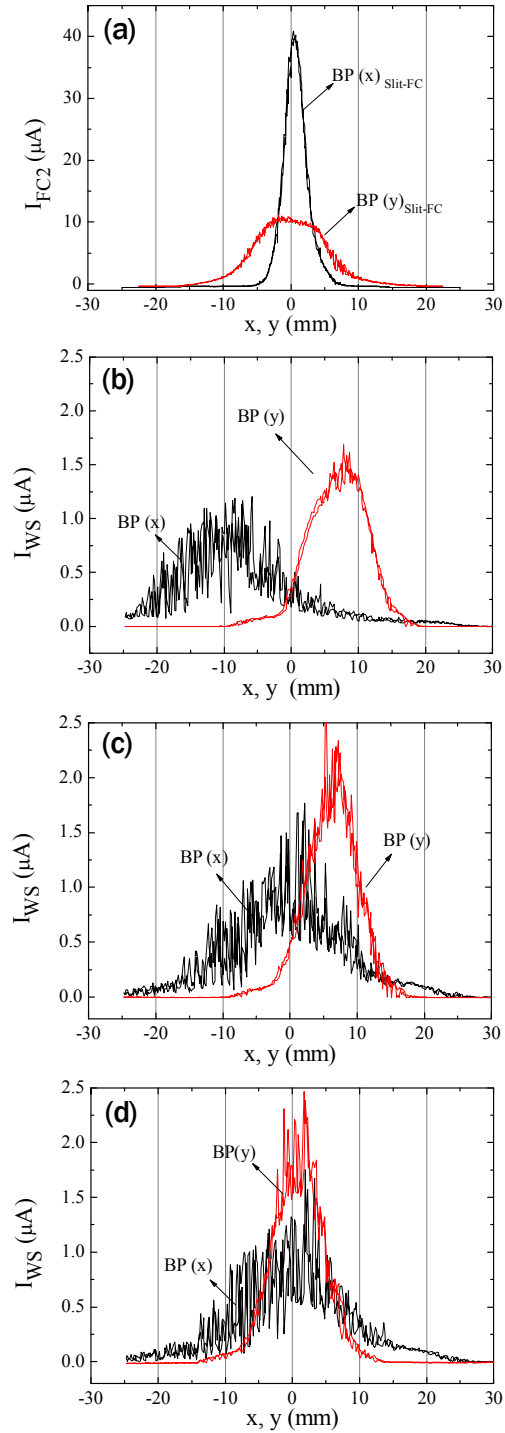


Figure 6: Horizontal (x) and vertical (y) beam profiles measured by (a) the Slit-FC system at MP1 and (b)-(d) the wire scanner at MP2: (b) not steered, (c) x-steered by ST1 (0.24 A), (d) y-steered by ST2 (1.2 A).

Figure 5: The slit-FC system and the wire scanner in the LEPT.

extracted with a source potential of 15 kV. The potential of Einzel lens 1 was tuned to -12 kV, so that the beam was well-focused at MP2 (SL 2 position). The steering magnet, ST1 is also finely tuned for the beam to be directed to the center region of the SL 2. Figure 6(a) shows the beam profiles at MP 1 measured by the slit-FC system. It is shown that x and y profiles are both well positioned at central region. Figure 6 (b)-(d) show the measured beam profiles by the wire scanner. The beam profiles (b), (c), and (d) were taken from three different steering conditions; Figure 6(b) is a beam profile that any further beam steering was not applied at all, Figure 6(c) is a beam profile that x- steering was applied by ST1, and Figure 6(d) is that for y-steering was done by ST2; In Fig. 6(c) and (d), the central positions of the beam were moved by 10 mm in x-direction, and by 6 mm in y-direction, meaning that beam steering has to be done to locate the beam to center region ($x, y=0$ at the position of MP 2). Dependence of beam profile on the Einzel lens 2 is shown in Fig. 7, where beam profiles were measured with different center electrode potentials ($V_{\text{einzel}}=-5, -15$, and -25 kV). As expected, it is observed that the higher potential(V_{einzel}) gives the better focusing effect resulting smaller beam width.

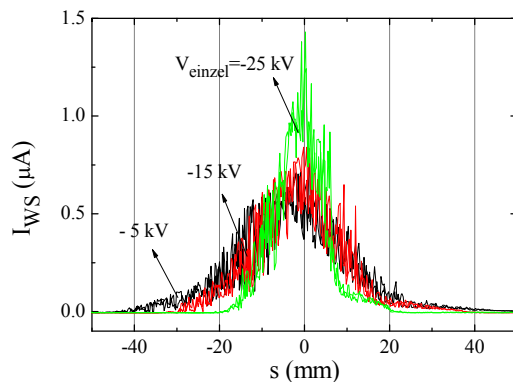


Figure 7: Measured beam profiles dependent on Einzel lens potential (V_{einzel}). The measurements are done at MP2 in diagonal(s) direction with the wire scanner.

First, in Fig. 6(a) showing the result of the slit-FC system, we can find that at MP1 horizontal(x) beam intensity is 4 times higher than vertical(y) beam intensity. It is thought that the smaller vertical(y) beam intensity comes from the unequal x and y dimension (132x52 mm) of the DM vacuum chamber. As shown by the envelop calculations in Fig. 3, the directed beam could be cut by the smaller height of the DM vacuum chamber. Secondly, from the comparison of the results from the slit-FC system and the WS, we see that at MP1 horizontal(x) beam profile is bigger and sharper than vertical(y) beam profile while at MP2 horizontal(x) beam profile becomes smaller and broader than y profile (compare Fig. 6(a) and (d)). This would mean that extracted beam could be rotated, which is possibly caused by the magnetic field gradient in extraction region (the axial magnetic field

drops from 1.3 T to 0 T within the extraction system); the decreasing field can give a beam rotation in azimuthal direction [4]. Thirdly, we found that beam steering is required in both side of the dipole magnet (before and after the DM); as compared the profiles from Fig. 6(a) to (d), aligning the beam at MP1 does not guarantee aligning the beam at MP2. In order to move the beams of MP1 and MP2 to each central region, one needs independent steering magnet such as ST1 and ST 2. Otherwise, the beamlines before and after the DM has to be carefully aligned. Lastly, the full widths at half maximum (FWHM) of Ar^{8+} were estimated that $\Delta x=3.5$ and $\Delta y=12$ mm at MP1, and $\Delta x=16$ mm ($\Delta y=9$ mm) at MP2, respectively.

CONCLUSION

As the first commissioning of SMASHI (the ECR ion source in NRFI), preliminary results of the beam charge spectra of ^4He , ^{16}O , ^{40}Ar , ^{132}Xe ion beams are obtained. So far, the maximum beam intensities of He^{2+} , O^{6+} , Ar^{8+} , and Xe^{20+} are recorded to be 1000, 200, 200, and 25 μA , respectively. Though all available operating knobs could not be used due to insufficient shielding of X-ray emissions, the present results show that SMASHI is a very promising source and its performance will be dramatically enhanced by applying higher microwave power(>1000 W/liter), higher magnetic field (>2 T), and higher extraction potential(>30 kV), etc. Then, with the beam profile measurements, we found that the LEBT transmission needs to be improved; in the present LEBT setup 1) very high beam losses are expected in front of the dipole magnet due to its small height of the inlet. Better matching of the ion beam to the dipole magnet is needed; 2) Beam steering is required in both side of the dipole magnet (before and after the dipole magnet). We also found in the beam profile measurements that the extracted beams could be experiencing a rotation. Lastly, measured full widths of half maximum of Ar^{8+} beam are estimated to $\Delta x=16$ mm $\Delta y=9$ mm at 116 cm from the exit flange of the dipole magnet.

ACKNOWLEDGMENT

The authors would like to gratefully acknowledge Dr. K. Y. Lee for his careful English proofreading and helpful comments.

REFERENCES

- [1] H. J. You, S. O. Jang, and W. I. Choo, Rev. Sci. Instrum. 85, 02A916 (2014).
- [2] H. J. You, S. O. Jang, Y.-H. Jung, T.-H. Lho, and S. J. Lee, Rev. Sci. Instrum. 83, 02A326 (2012)
- [3] H. J. You and K. M. Park, J. Supercond. Nov. Mag. 28, 651 (2015).
- [4] M. A. Leitner, D. C. Wutte, and C. M. Lyneis, Proc. 2001 Particle Accelerator Conference, 2001, Chicago, USA.